Delft University of Technology

State-of-the-art on impact and explosion behaviour of concrete structures
Report of RILEM TC 288-IEC

Cadoni, Ezio; Pérez Caldentey, Alejandro; Colombo, Matteo; Dancygier, Avraham N.; di Prisco, Marco; Grisaro, Hezi; Martinelli, Paolo; Ožbolt, Josko; Pająk, Małgorzata; Weerheijm, Jaap

DOI
10.1617/s11527-024-02557-x

Publication date
2025

Document Version
Final published version

Published in
Materials and Structures/Materiaux et Constructions

Citation (APA)
Cadoni, E., Pérez Caldentey, A., Colombo, M., Dancygier, A. N., di Prisco, M., Grisaro, H., Martinelli, P., Ožbolt, J., Pająk, M., & Weerheijm, J. (2025). State-of-the-art on impact and explosion behaviour of concrete structures: Report of RILEM TC 288-IEC. *Materials and Structures/Materiaux et Constructions*, *58*(2), Article 62. https://doi.org/10.1617/s11527-024-02557-x

Important note
To cite this publication, please use the final published version (if applicable).
Please check the document version above.

Copyright
Other than for strictly personal use, it is not permitted to download, forward or distribute the text or part of it, without the consent of the author(s) and/or copyright holder(s), unless the work is under an open content license such as Creative Commons.

Takedown policy
Please contact us and provide details if you believe this document breaches copyrights.
We will remove access to the work immediately and investigate your claim.

This work is downloaded from Delft University of Technology.
For technical reasons the number of authors shown on this cover page is limited to a maximum of 10.

Materials and Structures (2025) 58:62
https://doi.org/10.1617/s11527-024-02557-x

RILEM TC REPORT

State-of-the-art on impact and explosion behaviour of concrete structures: report of RILEM TC 288-IEC

Ezio Cadoni · Alejandro Pérez Caldentey · Matteo Colombo · Avraham N. Dancygier · Marco di Prisco · Hezi Grisaro · Paolo Martinelli · Josko Ožbolt · Małgorzata Pająk · Jaap Weerheijm

Received: 29 May 2024 / Accepted: 15 December 2024 / Published online: 7 February 2025
© The Author(s) 2025

Abstract Extreme loads can arise from accidents such as vehicle collisions or airplane crashes, as well as deliberate acts of terrorism or military attacks involving blasts and fragmentation. Blast overpressure can also occur accidentally, for example, from explosions of hazardous materials such as gas. Distinguishing between accidental and deliberate loads is crucial for designing appropriate protection measures. The repercussions of extreme loading events can be devastating, leading to injuries, loss of life, economic setbacks, and significant social disruption. These consequences result not only from the direct effects of impacts or explosions, but also from secondary factors such as structural collapse, which is particularly concerning due to its potential for widespread devastation and substantial losses. Efforts to enhance the protection of concrete structures have focused on understanding the properties of construction materials and how structures respond to impact and blast loads. This document presents a comprehensive overview of RILEM TC 288-IEC, aiming to provide essential guidance for designing concrete structures to withstand extreme dynamic loads. This emphasizes the importance of a thorough understanding and accurate modelling of loading scenarios and material behaviour. By implementing the strategies outlined in this document, engineers can enhance the safety and resilience of structures facing such challenges.

TC MEMBERSHIP: Marco di Prisco (chair), Ezio Cadoni (vice-chair): Giuseppina Amato, Nemy Banthia, Veronica Bertolli, Franz Bracklow, Alejandro Pérez Caldentey, Matteo Colombo, Manfred Curbach, Avraham Dancygier, Kazunori Fujikake, Hezi Grisaro, Terje Kanstad, Lena Leicht, Yann Malecot, Paolo Martinelli, Viktor Mechtcherine, Barzin Mobasher, Nikolaos Nikitas, Josko Ozbolt, Malgorzata Pajak, Prithvi Sangani, Amr Soliman, Francois Toutlemonde, Klaas van Breugel, Jaap Weerheijm.
This report was prepared within RILEM TC 288-IEC "Impact and Explosion" and subsequently circulated by the TC Chair for approval by TC members.

E. Cadoni
University of Applied Sciences and Arts of Southern Switzerland – DynaMat SUPSI Laboratory, Via Flora Ruchat-Roncati, 15, 6850 Mendrisio, Switzerland

A. Pérez Caldentey
Department of Mechanics of Continuous Media and Theory of Structures for the Civil Engineering, Universidad Politécnica de Madrid, C/del Prof. Aranguren, 3, 28040 Madrid, Spain

M. Colombo · M. di Prisco (✉) · P. Martinelli
Department of Civil and Environmental Engineering, Politecnico Di Milano, P. za L. da Vinci 32, 20133 Milan, Italy
e-mail: marco.diprisco@polimi.it

A. N. Dancygier · H. Grisaro
Faculty of Civil and Environmental Engineering, Technion - Israel Institute of Technology, 32000 Haifa, Israel

Keywords Impact · Explosion · Blast loading · Concrete structures · Strain rate · Mechanical properties · Structural behaviour

Abbreviations

CFD	Computational fluid dynamics
DIF	Dynamic increase factor
FE	Finite element
FRC	Fibre-reinforced concrete
HPFRCC	High-performance fibre-reinforced cementitious composite
HSC	High-strength concrete
SDOF	Single degree of freedom
SHPB	Split Hopkinson pressure bar
UHPC	Ultra-high-performance concrete

List of symbols

E	Young's modulus
$F(t)$	Force applied to a SDOF
$f_{c,imp,k}$	Characteristic uniaxial compressive strength under high rates of loading
f_{cm}	Mean value of uniaxial compressive strength of concrete
$f_{ct,imp,k}$	Characteristic uniaxial tensile strength under high rates of loading
f_{ctm}	Mean value of uniaxial tensile strength of concrete
f_{y}	Yield strength of reinforcing steel in tension
H	Distance from a reference explosion
i	Specific impulse
K	Spring stiffness
M	Lumped mass
$p_{\max}$	Peak pressure
R	SDOF system response
t	Time
t_{d}	Load time duration
t_{m}	Time corresponding to maximum response
$u, \dot{u}, \ddot{u}$	SDOF displacement, velocity and acceleration
W	Charge weight
Z	Scaled distance

Greek symbols

ε	Strain
ε_c	Concrete uniaxial compression strain
ε_{c1}	Concrete strain at maximum uniaxial compressive stress
$\varepsilon_{c1,imp}$	Impact concrete strain at maximum load in uniaxial compression
ε_{ct}	Concrete uniaxial tensile strain
ε_{ct1}	Concrete strain at maximum uniaxial tensile stress
$\varepsilon_{ct1,imp}$	Impact concrete strain at maximum load in uniaxial tension
$\dot{\varepsilon}$	Strain rate
$\dot{\varepsilon}_c$	Concrete uniaxial compression strain rate
$\dot{\varepsilon}_{ct}$	Concrete uniaxial tensile strain rate
σ	Stress
σ_c	Concrete uniaxial compression stress
σ_{ct}	Concrete uniaxial tensile stress
$\dot{\sigma}$	Stress rate
$\dot{\sigma}_c$	Concrete uniaxial compression stress rate
$\dot{\sigma}_{ct}$	Concrete uniaxial tensile stress rate
ω	Circular natural frequency

J. Ožbolt
Universität Stuttgart – Institute of Construction Materials, Pfaffenwaldring 4, 70569 Stuttgart, Germany

M. Pająk
Silesian University of Technology – Faculty of Civil Engineering, Akademicka 5, 44-100 Gliwice, Poland

J. Weerheijm
Delft University of Technology – Department of Civil Engineering and Geosciences, Postbus 5048, 2600 GA Delft, The Netherlands

1 Foreword

In the Development Advisory Committee (DAC) meeting held in Chennai in 2017, a key decision was made to strengthen the link between experimental laboratories, many of which possess specialized devices that are underutilized. This initiative aimed to reinvigorate the RILEM association, expanding its role beyond just an "Expert Link" to a "Labs Link," in line with its original mission to foster global collaboration and knowledge-sharing in the field of materials and structural research. Within the specific domain of impact and explosion, numerous experimental devices are available worldwide, often housed in military or research institutions. While access to some of these devices is restricted due to military ownership, many others are housed in universities or research centres and could contribute significantly to an international network, such as RILEM, for more effective utilization and cross-border collaboration. This collaboration would allow for the pooling of resources and expertise, enabling the sharing of critical data and findings related to the fast dynamic behaviour of construction materials—a field with relatively few specialists, but one that demands rigorous experimental validation and cross-comparison.

At the outset of this effort, the scientific community had yet to rigorously compare and validate results on high-strain material behaviour under dynamic loading, leading to significant uncertainty about the reliability and effectiveness of existing test methods. Therefore, the initial focus was on creating a solid foundation for progress by proposing the formation of a Technical Committee within RILEM to investigate the material parameters that characterize the high-strain behaviour of concrete structures. This led to the creation of RILEM TC 288-IEC in 2018, which brought together experts from the RILEM, fib, and ACI communities to address these gaps.

The main objectives of the Committee were as follows:

(1) To coordinate a database of special devices oriented to investigate the impact and explosion effects on materials and structures.
(2) To introduce the state-of-the-art knowledge in a specific fib bulletin that could work as a *fib* Model Code 2020 literature framework, aimed at guiding designers to quantify the bearing capacity of conventional structures to these specific actions.
(3) To propose and compare test methods to determine the parameters characterizing the high-strain behaviour of materials depending on the specific strain rate.
(4) To analyse the variables that most affect the structural response when subjected to these actions.
(5) To develop new practical recommendations and design criteria for structural members subjected to these phenomena.

The first goal was achieved through the creation of a comprehensive database of experimental devices, which catalogued 11 specialized devices from 11 countries. The mechanical characteristics, the problems investigated, the specific performance, the framework in which the device is operating, and the main references were summarized in detailed datasheets, which were made available to the RILEM community [1]. These devices were designed to study the high-strain rate behaviour of materials, and their inclusion in the database aims to facilitate collaboration and promote more effective use of underutilized equipment.

The following paragraphs of this report address objectives (2), (4), and (5). They explain the foundations of the background document, which will be published as a *fib* bulletin covering chapter 30.2.3 of the *fib* Model Code 2020 [2]. Additionally, they aim to integrate the knowledge of specialists in material behaviour and testing, primarily distributed among RILEM and ACI members, with the structural design knowledge prevalent among fib and ACI members.

In the meantime, a *fib* Special Activity Group (SAG) has been organized in a Working Parties (WP2.12.1—Design of structures subjected to impact and explosion), and the hope is that the cooperation between these three groups of experts could continue analysing objective (3) and that these results could be used to improve the basic knowledge required to further meet goals (4) and (5).

This report provides a general state-of-the-art aimed at providing essential guidance for designing concrete structures to withstand extreme dynamic loads, emphasizing the need for a comprehensive understanding and accurate modelling of loading scenarios and material behaviour.

2 Design strategies for RC construction under extreme dynamic loads

This document aims to outline strategies for designing reinforced concrete (RC) structures to withstand extreme dynamic loads, such as those from explosions, impacts, and projectiles. Particular attention is given to the material characterization and tests that may be instrumental in designing RC structures. Understanding this scenario is crucial for applying the design approaches discussed. Various scenarios are considered, including:

(1) Blasts caused by high explosives: load duration and pressure distribution depending on explosive type, amount, and boundary conditions. TNT equivalency and scaled distance approaches [3] can be utilized to define the load history [3, 4]. More complex approaches (e.g., computational fluid dynamics also considering fluid structure interaction) are instrumental for obtaining a more accurate description of the load.

(2) Gas explosions: the load history of the generated blast depends on the type of gas, the amount of gas, the confinement conditions, and the reaction mechanism (deflagration or detonation). Although TNT equivalence for gas explosions is suggested in the literature, it is not accurate because gas explosions have a much longer duration. Dedicated models, such as the multi-energy method [5], are available in the literature. A general overview of explosion mechanisms and modelling is provided in Van den Berg [6]. As discussed in the previous scenario, a more comprehensive description of the load history and pressure distribution over the structure can be achieved through more complex approaches, such as computational fluid dynamics (CFD) analysis.

(3) Impact loads: different from blasts due to longer duration and localized application, impacting objects strike structures, requiring consideration of object mass, stiffness, velocity, and protective measures. Several codes (such as Eurocode EN 1991–1-7 [7]) provide definitions of the load history. Even in this case, advanced numerical analysis can be adopted to provide a more complete prediction of the phenomenon.

(4) Fragmentation and projectiles: this scenario refers to structures that can be hit by projectiles, often generated by blast phenomena that create fragments travelling in the air at very high velocity; the investigation of this scenario, due to the complex nature of the phenomenon, requires advanced analysis.

(5) Fire and blast events: in some situations, blast events can be preceded by fire; under such conditions, the structure responds to blast loads when damaged by fire. An uncoupled approach between the two actions can be adopted in terms of load, but the damage caused by fire has to be considered when investigating the resistance to a blast load. Even in this case, more advanced numerical approaches can be instrumental to truly consider the interaction between the two phenomena.

Similar to *fib* Bulletin 63 [8] and other documents in the scientific literature, this report provides a broader overview of the design of RC structures for extreme actions, focusing not only on global structural integrity, but also on element resistance to specific loads.

The response of structures to dynamic loads depends on parameters related to both the structure and the load. There is a strong correlation between the natural frequency of the structural system and the duration of the applied load [9–11]. Structural responses can be categorized into impulsive, dynamic, and quasi-static regimes based on the load duration and the natural frequency of the structure [4]. In the case of the quasi-static regime, the load duration is considered “long” if the duration of its peak (or near-peak) value is similar to or longer than the time it takes for the structure to reach its maximum response. In this regime, the maximum response of the system depends only on the maximum applied load and structural stiffness. In contrast, in the impulsive regime, the load duration is so short that the system reaches its maximum response when the load is (almost) over. In this regime, the maximum response of the systems is governed by the impulse of the load history. The third transition regime, defined as the dynamic regime, generally lies between the impulsive and quasi-static regions. In this regime, the loading duration and the system response time are comparable. In this regime, the response history is more complex and significantly influenced by the profile of the load history. A schematic view of the definitions of the different regimes is provided in Fig. 1.

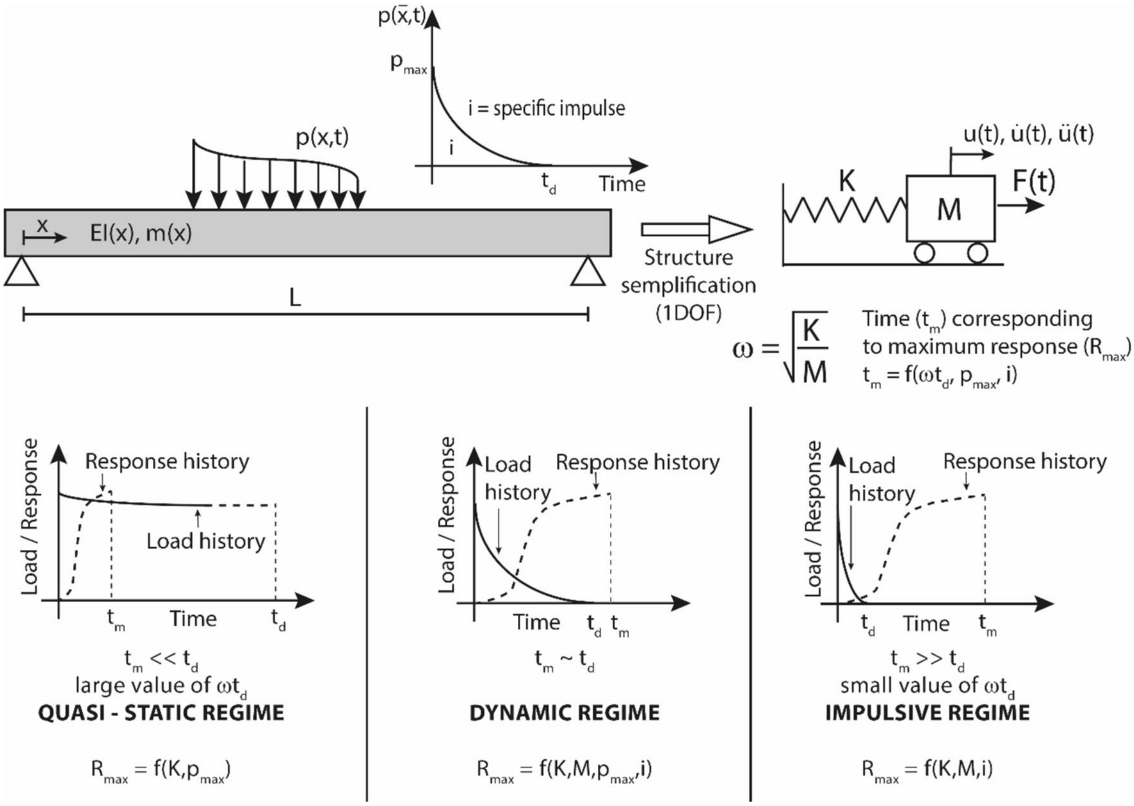

Fig. 1 Structural response regimes for a structure simplified with a Single Degree of Freedom System

Loading rates significantly influence material and structural responses [12–26], primarily through microstructural effects, material viscosity, and inertia effects at meso- or macro-scales [27, 28]. A more detailed analysis of the strain rate effect on the material is provided in the following sections.

International design standards classify buildings based on the potential consequences of collapse, guiding the adoption of appropriate design strategies. Eurocode EN 1991–1-7 [7], for instance, categorizes buildings into three consequence classes:

(1) Consequence Class 1: buildings with low or limited consequences, such as single occupancy houses or agricultural structures, generally require no specific considerations regarding accidental actions.
(2) Consequence Class 2: buildings with medium consequences are further subdivided into categories 2a and 2b based on size and occupancy. Design strategies for this class include an indirect approach focusing on enhancing structural robustness and continuity for class 2a buildings. Class 2b buildings require more rigorous design considerations, such as alternative load path approaches and specific load resistance methods.
(3) Consequence Class 3: buildings with high consequences, including those exceeding the size and occupancy limits of class 2, require a systematic risk assessment considering both foreseeable and unforeseeable hazards.

Similarly, in the United States, the Department of Defense (DoD) delineated four levels of protection (later replaced by occupancy categories) in their Unified Facilities Criteria (UFC), ranging from a very low level of protection to a high level of protection [29].

The design strategies vary according to the consequence class:

(1) Indirect Design Approach: this approach focuses on enhancing structural robustness through prescribed tie systems, ensuring continuity and force redistribution within the structure.
(2) Alternative Load Path Approach: this approach assumes that a portion of the structure is damaged and focuses on redistributing loads to undamaged elements. Dynamic effects and alternative resistance mechanisms are considered.
(3) Specific Load Resistance Method: this method involves explicitly designing structural elements to resist a defined load condition, necessitating detailed scenario definition and analysis.
(4) Mitigation of Action: this method involves various approaches to mitigate the effects of accidental actions, such as protective barriers, crushable materials, and architectural layout considerations. For example, convex shapes are preferred over re-entrant corners to minimize load amplification from blast waves.

3 High strain rate behaviour of the material

The response of reinforced concrete structural elements to dynamic loading is influenced by the mechanical behaviour of both the concrete and reinforcing steel under dynamic conditions. These elements typically exhibit greater load-bearing capacity than under quasi-static loading scenarios because the material strength increases with increasing stress or strain rates. This stress or strain rate sensitivity is crucial to consider in the design of reinforced concrete structures exposed to significant dynamic loads.

Various materials used in these structures, such as plain concrete, fibre-reinforced cementitious composites, and reinforcing steel, demonstrate positive sensitivity to stress or strain. Of particular importance in design considerations are the compressive and tensile strength of concrete, as well as the yield and ultimate tensile strength of reinforcement bars.

The loads resulting from impact and explosions are characterized by high dynamic loads with strain rates significantly higher than those, for example, of traffic or earthquake loads [30], as schematically illustrated in Fig. 2.

The determination of stress and strain is contingent upon the specific point and direction under analysis. As a result, concepts related to strain or stress rates also exhibit this dependency. These rates are defined by their changes over time. To assist designers in interpreting material characterization data, the following key points are provided.

The strain and stress rates (Fig. 2) in the unidirectional case are defined as follows:

$$\dot{\varepsilon} = \frac{\partial \varepsilon}{\partial t} \tag{1}$$

$$\dot{\sigma} = \frac{\partial \sigma}{\partial t} \tag{2}$$

In the elastic field, the Hooke law is valid, and with the hypothesis that the elastic modulus E does

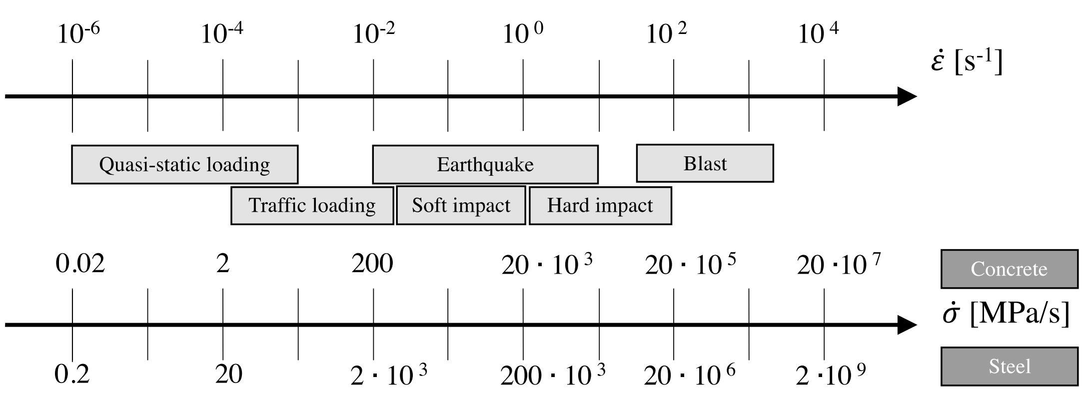

Fig. 2 Elastic strain-rates for different loading velocities [17, 31] and correspondent stress-rates. *Note*: in the figure elastic modulus for concrete is considered equal to 20 GPa while 200 GPa for steel

not vary as a function of time, the stress and strain rate are obtained as follows:

$$\dot{\sigma} = \frac{\partial(E \cdot \varepsilon)}{\partial t} = \frac{E \cdot \partial(\varepsilon)}{\partial t} = E \cdot \dot{\varepsilon} \tag{3}$$

As a result, two values can be obtained in tests from measurements of the specimen: the first is the slope of the stress vs. time curve in the elastic field, and the second is obtained by dividing the stress rate by the elastic modulus.

When elasto-plastic analysis is needed, the plastic strain rate must be considered. The strain rate in the plastic domain, in the case of reinforcing steel or in strain hardening fibre-reinforced cementitious composites, is widely adopted as the average value of the hardening phase [32–35]. For quasi-brittle materials (with softening behaviour) such as plain concrete, the plastic strain rate refers to irreversible components. It can be measured in correspondence with the maximum strength or if a plateau is obtained as an average of the strain rate at the plateau. Note that the strain rate in the hardening and softening regime depends on the measured/considered width of the failure zone.

3.1 Experimental techniques used for determining the rate influence on materials

The rate-dependent material properties of concrete are investigated by using advanced experimental techniques and can be categorized into four main groups:

(1) Servo-hydraulic machines: these methods subject the specimen to applied loading, strain, or deflection rates. They provide insights into concrete behaviour under quasi-static and moderate strain rates, typically up to 10^{-4} s^{-1}. Various tests, such as compression, tension and flexure, can be carried out on different types of specimens using this approach. (Equipment available at lab 2 and 6 of the "RILEM report on Experimental devices harvest for impact and explosion testing of materials and structures" [1]).

(2) Drop-weight impact machines: these machines involve striking concrete beams or slabs under high strain rates using a falling mass. Drop towers with adjustable masses can apply impacts ranging from a few kilograms to several tons, with heights up to 10 m. Load−displacement curves are obtained from these tests, which provide information about the concrete behaviour at strain rates ranging from 10^{-3} s^{-1} to 10 s^{-1}. Accelerometers are often used to record midspan deflection during these tests. (Equipment available at lab 4, 6 8 and 11 of the "RILEM report on Experimental devices harvest for impact and explosion testing of materials and structures" [1]).

(3) Air-gun-based tensile impact machines: in this method, projectiles of various shapes are launched via air or gas guns to impact concrete plates of different depths. This test assesses the resistance of the concrete plate to projectile damage, measured by parameters such as crater diameter, penetration depth, and weight loss. (Equipment available at lab 7 of the "RILEM report on Experimental devices harvest for impact and explosion testing of materials and structures" [1]).

(4) Split Hopkinson pressure bar (SHPB) testing: this technique evaluates concrete behaviour under compression and tension by sandwiching the specimen between two bars. A one-dimensional stress pulse is generated and propagated through the bars, allowing for the calculation of the stress, strain, and strain rate in the specimen. SHPB tests provide stress−strain curves and strain rates for concrete under high strain rates, typically ranging from approximately 10^1 to $5{\cdot}10^2$ s^{-1} for compression and from 0.1 to $0.2{\cdot}10^2$ s^{-1} for tension. Modifications of the SHPB technique enable the investigation of concrete in biaxial and triaxial stress states. (Equipment available at labs 2, 3, 4, 5, 6, 9 and 10 of the "RILEM report on Experimental devices harvests for impact and explosion testing of materials and structures" [1]).

Additionally, shock tube equipment or blast simulators can be used to test material performances under high strain rates even if they are more suitable for testing the structural response of full- or small-scale structural elements. (Equipment available at laboratories 1, 3 and 7 of the "RILEM report on Experimental devices harvest for impact and explosion testing of materials and structures" [1]).

A detailed description of various experimental methods for testing materials and structures under impact and blast conditions is also provided in

Chapter 3 of ACI 544.E document [36] and in [37]. A specific description of the testing devices used to identify the main mechanical properties involved in the response of concrete under dynamic tensile loading is given in [38].

3.2 Rate-dependent properties of concrete related to impact and explosion

Recent codes, such as *fib* Model Code 2020 [2], propose formulations to compute the rate effect on material properties. These relations are valid for monotonically increasing compressive stresses or strains at a constant range of approximately 1 MPa/s < $|\dot{\sigma}_c| < 10^7$ MPa/s and $30{\bullet}10^{-6}$ s^{-1} < $|\dot{\varepsilon}_c| < 3{\bullet}10^2$ s^{-1}, respectively. In the corresponding equations, all the strain and stress values are used in terms of their absolute values. For tensile stresses or strains, the information is valid for approximately 0.03 MPa/s < $|\dot{\sigma}_{ct}| < 10^7$ MPa/s and $1\cdot10^{-6}$ s^{-1} < $|\dot{\varepsilon}_{ct}| < 3{\bullet}10^2$ s^{-1}, respectively.

The following expressions are recommended to be used in fully dynamic analyses of concrete structures. The proposed relationships are valid for standard concrete with strengths ranging from 30 to 60 MPa, which are most frequently used in engineering practice. Further explanation regarding the use of these expressions is given in the next sections and in the commentary column of the *fib* Model Code 2020 in the Sect. 14.6.2.2 titled "Properties related to impact and explosion" [2].

3.2.1 *Compressive strength*

For a given strain and stress rate, the compressive strength under high rates of loading ($f_{c,imp,k}$) may be estimated as:

$$f_{c,imp,k}/f_{cm} = \left(\dot{\varepsilon}_c/\dot{\varepsilon}_{c0}\right)^{0.014} \tag{4}$$

with $\dot{\varepsilon}_{c0} = 30\cdot10^{-6}$ s^{-1} and

$$f_{c,imp,k}/f_{cm} = \left(\dot{\sigma}_c/\dot{\sigma}_{c0}\right)^{0.014} \tag{5}$$

with $\dot{\sigma}_{c0} = 1$ MPa/s.

In Eqs. (4) and (5), $\dot{\varepsilon}_c$ represents the compressive strain rate in s^{-1}, f_{cm} is the mean compressive strength in MPa and $\dot{\sigma}_c$ is the compressive stress rate in MPa/s.

3.2.2 *Tensile strength and fracture properties*

For a given strain and stress rate, the tensile strength under high rates of loading ($f_{ct,imp,k}$) may be estimated as:

$$f_{ct,imp,k}/f_{ctm} = \left(\dot{\varepsilon}_{ct}/\dot{\varepsilon}_{ct0}\right)^{0.018} \tag{6}$$

with $\dot{\varepsilon}_{ct0} = 1{\bullet}10^{-6}$ s^{-1} and

$$f_{ct,imp,k}/f_{ctm} = \left(\dot{\sigma}_{ct}/\dot{\sigma}_{ct0}\right)^{0.018} \tag{7}$$

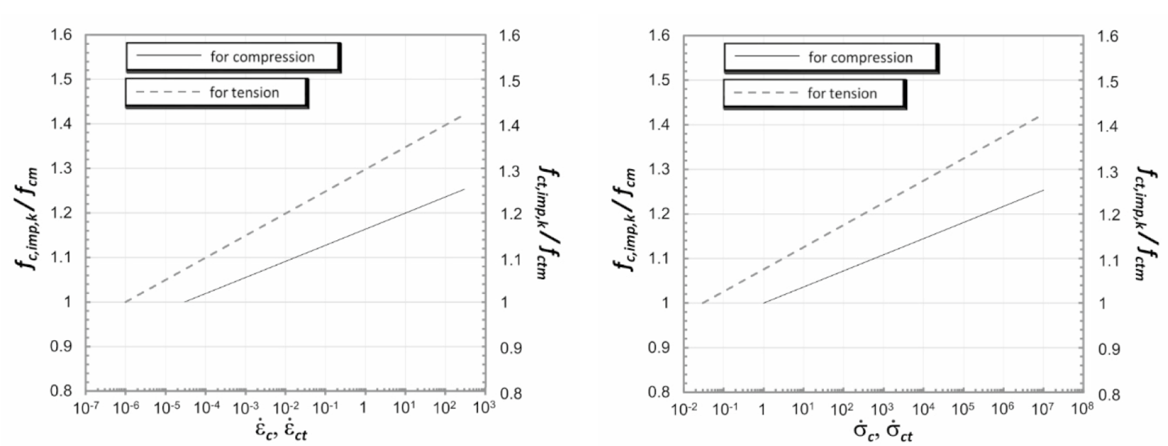

(a) (b)

Fig. 3 Effect on compressive and tensile strength of concrete of **a** strain-rate and **b** stress-rate with $\dot{\sigma}_{ct0} = 0.03$ MPa/s.

In Eqs. (6) and (7), $\dot{\varepsilon}_{ct}$ represents the tensile strain rate in s^{-1}, f_{ctm} is the mean tensile strength in MPa and $\dot{\sigma}_{ct}$ is the tensile stress rate in MPa/s.

The increase in the compressive and tensile strengths of the concrete with increasing strain/stress rate determined from Eqs. (4)–(7) is presented in Fig. 3.

Note that the rate dependency in the *fib* Model Code [2], and Eqs. (4)–(7), is represented with a single branch in the semi-logarithmic scale. No enhanced rate dependency for high loading rate regimes is given. In dynamic compression or tensile tests, an enhanced strength increase is observed beyond a certain loading (strain) rate. The mechanisms causing this observed rate dependency have been studied over the last few decades, and a common agreement on these mechanisms has been reached. Inertia affects damage development/the fracture process at all scales, from the micro and meso scale up to the macro scale of the structural response. The time-dependent response is also influenced by viscous effects due to the water in the pores. Thus, the rate-dependent response of concrete specimens is based on the material response across a range of length scales driven by inertia and viscosity. In the literature, there is ongoing discussion about which part of the observed strength increase should be included in the constitutive law and which part is automatically covered by advanced numerical modelling. This depends on the level of detail, the scale of modelling, and the type of model applied (plasticity, damage, or micro-plane model, as discussed in Sect. 3.5). In the *fib* Model Code [2], viscous effects and the initial damage growth at the micro scale are included in the constitutive law, represented by a single branch in the semi-logarithmic scale. Other mechanisms should be addressed by numerical modelling itself. If this is not the case, the missing effects should be incorporated into the constitutive law of the applied material model. Clearly, modelling the dynamic response of concrete and concrete structures is a challenging task.

3.2.3 *Fracture energy*

The available information on the effect of stress or strain rates on fracture energy is too incomplete to be discussed in this document. The results in the literature do not clearly indicate whether the fracture energy increases or decreases as the strain rate changes. Moreover, it is important to note that only the total fracture energy can be measured without distinguishing between its various components.

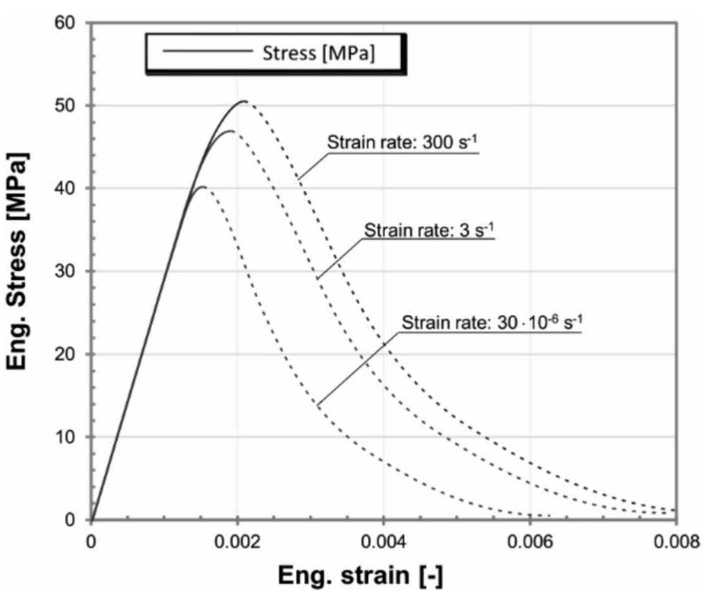

Fig. 4 Illustration showing the strain-rate effect on the stress−strain behaviour of concrete under compression. The maximum stress and corresponding strain were determined using Eqs. (4) and (8)

3.2.4 Modulus of elasticity

The available experimental data indicate that the modulus of elasticity of concrete is unaffected by the stress or strain rate [39, 40].

3.2.5 Strain at peak stress

The effects of high stress and strain rates on the strains at maximum stress in compression and tension, $\varepsilon_{c1,imp}$, $\varepsilon_{ct1,imp}$, may be estimated as:

$$\varepsilon_{c1,imp}/\varepsilon_{c1} = \left(\dot{\sigma}_c/\dot{\sigma}_{c0}\right)^{0.02} = \left(\dot{\varepsilon}_c/\dot{\varepsilon}_{c0}\right)^{0.02} \tag{8}$$

$$\varepsilon_{ct1,imp}/\varepsilon_{ct1} = \left(\dot{\sigma}_{ct}/\dot{\sigma}_{ct0}\right)^{0.02} = \left(\dot{\varepsilon}_{ct}/\dot{\varepsilon}_{ct0}\right)^{0.02} \tag{9}$$

with $\dot{\sigma}_{c0} = 1$ MPa/s and $\dot{\varepsilon}_{c0} = 30{\bullet}10^{-6}$ s^{-1} for compression and with $\dot{\sigma}_{ct0} = 0.03$ MPa/s and $\dot{\varepsilon}_{ct0} = 1{\bullet}10^{-6}$ s^{-1}for tension. In Eqs. (8) and (9), ε_{c1} and ε_{ct1} represent the strains at the maximum load for quasi-static loading for uniaxial compression and tension, respectively.

An example of the strain rate effect on the stress–strain behaviour of concrete under compression is presented in Fig. 4, where the maximum stress and corresponding strain were determined based on Eqs. (4) and (8).

3.3 Rate-dependent properties of fibre-reinforced concrete/HPFRCC/UHPC

Cement-based materials reinforced with randomly distributed short fibres, such as fibre-reinforced concrete (FRC), high-performance fibre-reinforced cementitious composite (HPFRCC), and ultra-high-performance concrete (UHPC), exhibit strain/stress-rate sensitivity, with the type of fibre playing a crucial role in this sensitivity. The response of these materials to high dynamic loadings depends on factors such as the fibre volume fraction, type, length, and other geometrical parameters. Generally, the addition of fibres to the concrete matrix reduces the strain rate sensitivity compared to that of plain concrete [41–45].

However, the strength enhancement resulting from increased stress/strain rates in fibre-reinforced cement-based materials needs to be experimentally validated for each specific case before being incorporated into engineering practice.

A comprehensive overview of the experimental campaign on FRC materials is provided by ACI 544.E [36] provided several examples of materials tested and even formulations for the computation of FRC mechanical performance with increasing strain rate.

3.4 Rate-dependent properties of reinforcing steel

The equations describing the dynamic increase factor (DIF) formulation for the yield and ultimate stress of reinforcing steel (Fig. 5) are provided in Eqs. (10)-(12) and can be found in [46]:

$$\mathrm{DIF} = \left(\frac{\dot{\varepsilon}}{10^{-4}}\right)^{\alpha} \tag{10}$$

For the yield stress, $\alpha = \alpha_{fy}$ is determined by:

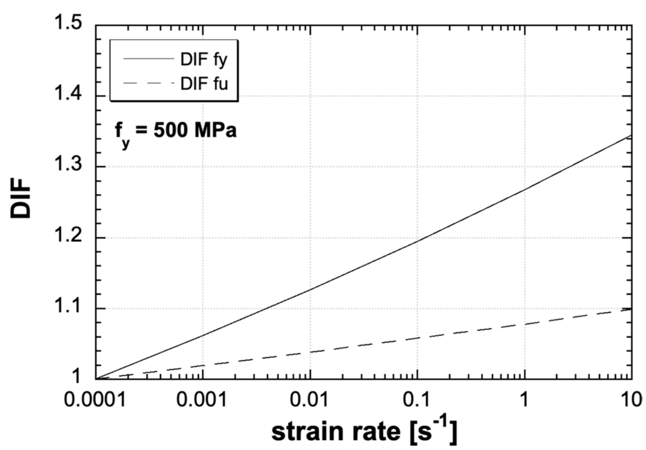

Fig. 5 Increase of reinforcing steel strength as a function of strain rates

$$\alpha_{fy} = 0.074 - 0.040\left(\frac{f_y}{414}\right) \quad (11)$$

and for the ultimate stress, $\alpha = \alpha_{fu}$ is determined by:

$$\alpha_{fu} = 0.019 - 0.009\left(\frac{f_y}{414}\right) \quad (12)$$

Here, f_y represents the yield strength of the reinforcing bar in MPa. This formulation applies to reinforcing steel with yield stresses ranging from 290 to 710 MPa and strain rates between 10^{-4} and 10 s^{-1}. Various experimental data at higher strain rates can be found in [33, 34, 47], as well as when combined with elevated temperatures [48–50].

3.5 Evaluation of the DIF and its applicability to prevent overestimation of the resistance

Understanding the dynamic fracture behaviour of concrete under high strain rates is fundamental for ensuring the safety and integrity of concrete structures subjected to dynamic loading, such as impact and blast events. Compared with quasi-static conditions, concrete exhibits distinct responses under dynamic loading, primarily due to the influence of strain rate effects on its mechanical properties and the activation of inertia [24, 51].

The experimental results showed that the concrete resistance progressively increased with increasing loading rate across the various loading scenarios. This increase in resistance is observed in compression, direct tension, bending, and other loading modes. Although each experimental method has its limitations, they collectively demonstrate an increase in the concrete resistance under dynamic loading [52–62].

To quantify the strength enhancement resulting from strain rate effects, researchers have introduced the DIF, which represents the ratio of dynamic to static resistance. However, the scatter in DIF data highlights the complexity of dynamic material behaviour, influenced by a multitude of parameters, including material properties and structural effects [58, 59, 63–67].

The progressive increase in resistance with increasing loading rate is attributed to various factors, including structural inertia, crack propagation, and other macroscopic effects. Structural inertia refers to the inertia generated by the movement of the specimen, which impacts its overall resistance. Additionally, changes in failure modes under dynamic loading, such as the transition from mode-I to mixed-mode or shear failure, further complicate the assessment of concrete resistance.

When applying DIF in structural design or analysis, it is essential to consider the dynamic failure mode and its potential impact on the overall resistance. While DIF accounts for the effects of material microstructure in the constitutive law, it is crucial to recognize that inertia effects occur at all material scales and also vary based on the structure size and type. The response at the larger scales may be covered by detailed numerical modelling. Therefore, a cautious approach is warranted to avoid overestimation of inertia effects and ensure the reliability of structural designs under dynamic loading conditions. Alongside these inertia effects, one should also consider the classical contributions of the size effect.

The main reason for the progressive increase in resistance with increasing loading rate is the activation of inertia at the macro-scale, which is due to different reasons, such as structural inertia, inertia due to the hardening or softening of concrete, crack propagation and crack branching [24, 51, 68]. Note that structural inertia refers to the structural response of the specimen. For example, in the case of a concrete cylinder in compression, it is the inertia generated due to lateral material displacements in the specimen. The specimen is unable to expand freely in the lateral direction due to inertial restraint, resulting in lateral stresses that act as a form of confinement [66]. When modelling structures at the meso- or macro-scale, these effects are automatically accounted for in a sufficiently detailed numerical analysis (see, for example, [24]), whereas the rate effect coming from the material micro level must be covered by the constitutive law. On the contrary, in tension modelling, crack initiation, propagation, and branching in dynamic conditions appear to depend not only on the level of modelling detail, but also on the material model itself. For example, the micro-plane model [24, 25, 28, 38] seems to be very effective in capturing inertia effects from the meso- to the macro-scale. Therefore, the observed enhanced strength increase at high rates should not be included in the constitutive law, the DIF. In contrast, plasticity and damage models appear to be less effective in covering the inertia effects of the fracture process, so the enhancement of material strength must be included in the constitutive law. In [38], researchers present different modelling techniques, all capable of adequately reproducing experimental results but with different DIF functions to adjust the (static) constitutive law. Obviously, modelling the dynamic response of concrete and concrete structures is a challenging task and requires caution due to the following important considerations, as discussed below.

Accounting for increased resistance in structural design can involve incorporating DIFs to reflect the apparent strength of materials, such as compressive and tensile strength. An example is the design of concrete columns loaded in compression, where lateral confinement due to structural inertia enhances compressive resistance. However, implementing this approach requires caution due to two important considerations, as discussed below.

First, comparing rate-sensitive constitutive laws directly with dynamic test results is problematic. Dynamic failure surfaces cannot simply be derived by multiplying static failure surfaces by corresponding DIFs obtained in tests. Instead, tests should be compared with numerical simulations to isolate inertia effects. The adoption of quasi-static constitutive laws based solely on dynamic test results for specific geometries is misleading, as dynamic test outcomes are heavily influenced by specimen geometry. It is important to filter out the effects of inertia from the constitutive law, as they can lead to an overestimation of the impact of inertia in structural analysis. In tension, the result of the filtering depends on the applied material model and the level of modelling detail. The DIF function to be applied can range from the very extreme of the apparent strength in the tests (the old CEB-FIP equations [63]) to the single branch function in the model code [2].

Second, the application of DIF in structural design must consider how the loading rate affects failure modes. Increased loading rates often cause transition mode-I failure to form mixed-mode or shear failure.

Considering these two aspects, DIF must be carefully applied in the design or analysis of structures. As already stated, the effects coming from the microstructure of the material must be accounted for in the constitutive law (e.g., DIF on compressive or tensile strength); however, the inertia effects coming from the macro scale (progressive increase in resistance) are very much dependent on the type of structure and its size. This means that in relation to a specific test adopted to identify the dynamic constitutive law and with reference to a specific structural model, it is important to calibrate the DIF value to suitably simulate the experimental response.

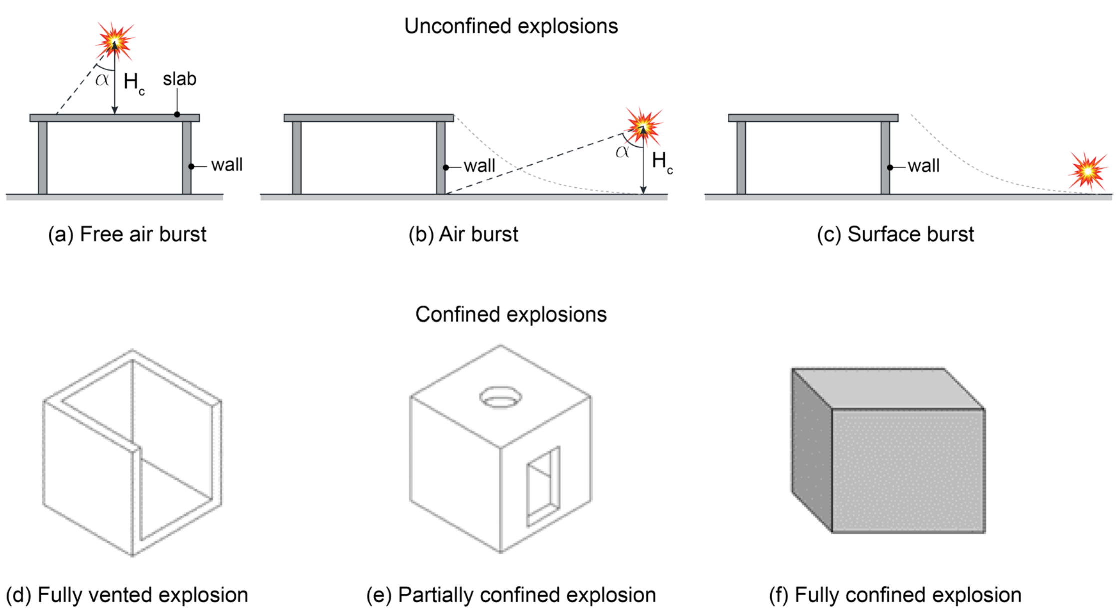

Fig. 6 Blast-loading categories

4 Types of analyses

4.1 Blast actions

Blast analyses are paramount for evaluating the structural response to explosions. These analyses encompass various methodologies tailored to different types of explosions. The categorization is based on whether the explosion is confined within a structure or unconfined outside it, each requiring specific analytical approaches (Fig. 6).

(1) Unconfined Explosions: these explosions occur outside the structure, exerting blast loads directly on external walls or slabs. Unconfined explosions can be further classified into three subcategories:

   a. Free air burst: in this scenario, the explosion occurs without ground reflection, and the structure receives the blast load directly. The pressure at each point is determined by the perpendicular distance to the explosion surface (Hc) and the incidence angle (α).
   b. Air burst: this explosion occurs at a limited height above the ground, with the blast wave reflected by the ground, forming a Mach front. The pressure wave is relatively constant along the height of the Mach front.
   c. Surface burst: originating from the ground, the explosion leads to a uniform load along the structure height, depending on the horizontal distance between the blast load and the structure.

(2) Confined Explosions: confined explosions occur within a structure, and their effects can be intensified by reflections on different structural elements. They can be further subcategorized as follows:

   d. Fully vented explosion occurs when there are no solid elements in at least one direction, amplifying the explosion effects.
   e. Partially confined explosion occurs within a structure with limited openings, leading to the generation of high temperatures and gaseous products.
   f. Fully confined explosion: shock loads and long-duration gas pressures within the structure.

Considering this categorization of action, the following types of analysis can be considered:

(1) Simplified quasi-static analysis for unconfined explosions: this analysis simplifies the pressure−time wave into a triangular law, determines the first period of vibration of the structure, and calculates the dynamic load factor (DLF). The process involves:

   a. Simplification of the pressure−time wave into a triangular law. The main parameters of this pressure history are the maximum pressure at the arrival time and the specific impulse. These parameters are defined according to the formulation proposed in the literature [3, 69] and depend on the scaled distance (Z) defined according to equation (13):

$$Z = \frac{H}{W^{1/3}} \tag{13}$$

   where W is the TNT equivalent weight and H is the distance between the target structure and the explosion source.
   b. Determination of the structure first period of vibration by assimilating it to a single-degree-of-freedom (SDOF) system.
   c. Calculation of the DLF based on the ratio of the duration of the equivalent triangular load to the structure first period of vibration.
   d. Application of equivalent loads on the structure and verification of structural integrity using plastic analysis.

(2) Finite element (FE) analysis based on pressure–time curves: some FE codes [70] allow for the automatic generation of blast loads based on pressure–time diagrams. However, this method becomes less precise when the distance from the blast load to the reflecting element is smaller than 0.5 m.
(3) Finite element analysis based on the simulation of pressure waves: this approach utilizes compu-

tational fluid dynamics [70–72] to simulate pressure waves and requires fine discretization and detailed explosive characterization. However, this approach can be resource intensive, especially for large models.

A very useful approach in the design of structural elements subjected to explosions is the pressure–impulse (p–i) diagram, which allows the designer to verify the safety of the structure by referring to a well-defined limit state with respect to a wide range of load scenarios [3, 4, 73–75]. P-i curves are a series of iso-damage curves that provide a graphical representation of the structural response in terms of pressure and impulse values. This method enables the determination of the pressure/impulse values that cause a certain level of damage to the structure and facilitates comparison with the structural capacity to ensure structural safety. P–i diagrams can be generated analytically or numerically; in the latter case, a large number of pressure and impulse combinations are required to generate a reliable damage curve.

In summary, evaluating structural response under explosive loads requires the application of diversified methodological approaches and the adoption of compromises between accuracy and analytical complexity. Although each method has advantages and limitations, integrating multiple techniques can provide a more comprehensive and reliable assessment of structural safety in explosion scenarios.

4.2 Impact actions

Referring to impact actions, in simplified terms, these problems can be divided into two types: soft impact and hard impact. Soft impact occurs when the impacting body experiences deformations that are significantly greater than the deformations of the impacted structure. Typical cases of soft impact include car crashes and aircraft fuselage impact. Hard impact occurs when the impacting body is rigid, and its deformations are negligible with respect to the deformations of the impacted structure.

A simplified model for impact can be conceived as developed in the literature [76]. For this, a two-mass and two-degree-of-freedom system can be considered. The first mass (m_1) and displacement (x_1) represent the impacting element (projectile), while the second mass (m_2) and displacement (x_2) represent the impacted element (structure). Both the impacting mass and structure have their corresponding stiffnesses (K_1 and K_2), which can be nonlinear. The method applies the dynamic equilibrium equations to the two systems assuming an initial velocity for the impactor.

When considering the structural response under soft impact, the local behaviour is generally not important. The relevant analysis in these cases is the global structural analysis. Modelling of soft impact using FE analysis is quite straightforward since local damage to the structure is not an issue. The problem is reduced to applying a localized impulse on the structure. The microscopic strain rate effects are not expected to be significant since the transmission of the strain waves is governed by the natural period of the structure. All macroscopic strain-rate effects come, of course, directly from dynamic analysis and need not be accounted for separately.

Under hard impact, most of the emphasis is placed on local behaviour, mainly penetration (the depth of the protective structure that the projectile passes through before stopping), perforation, which is the worst-case scenario of penetration, spalling (the crater the projectile leaves on the side of impact and/or material fragments that detach from the inner, protected face) and scabbing (which is spalling occurring on the inside of the protected structure due to partial penetration of a projectile).

Analysis of hard impact actions can be carried out at different levels:

- Empirical formulations.
- Simplified axisymmetric penetration model [77].
- Nonlinear FE analysis.

When conducting finite element simulations to model high-impact scenarios, according to Irhan [78], it is crucial to consider strain rate effects, which arise from various phenomena at different scales. At the microlevel, inertia reduces the formation of microcracks as the strain velocity increases, and according to [78], it influences the constitutive law of materials such as concrete. Additionally, the bulk material behaviour between cracks exhibits rate effects due to viscosity, possibly caused by heat generation or comminution during penetration. At the macroscopic level, strain rate dependency arises from inertial effects during dynamic analysis and does not need to be incorporated into material constitutive laws if a sufficiently detailed numerical analysis is employed (see, for example, [24]), as it depends on the level of detail and type of modelling. Depending on the applied material model and the level of detail of the numerical analysis, the constitutive law is adjusted to capture the rate dependency correctly, (see Sect. 3.5).

Another significant consideration in high-stress modelling is preventing premature termination of calculations due to local finite element failure. A commonly used technique is element removal, which is performed with software such as LS-Dyna. Some authors [78] suggest removing elements when the maximum principal strain reaches 1.00, which is particularly relevant in penetration problems where material disintegration facilitates penetration.

4.3 Combined effects of explosions and fragments

In the design and analysis of structures under extreme loads, scenarios involving detonations of explosive charges enclosed by metal casings are common. These scenarios produce both pressure waves and fragments flying at high velocities, potentially impacting structural elements. Fragments are typically generated from casing breakage, while pressure arises from the explosion and its reflection within the structure. The arrival times of fragmentation and pressure waves at a structure differ due to varying velocities. Fragments typically reach the structure after pressure waves over short distances, but may coincide or precede pressure waves over longer distances [79, 80]. This timing discrepancy can lead to interactions between the two effects, potentially exacerbating damage. The combined loading of blast and fragments results in three main effects: damage from fragment impacts, impulse on the structure due to fragments, and impulse due to blast loading. The rupture of the metal casing generates additional damage and impulses from fragments, while the effectiveness of the blast may decrease due to energy dissipation during casing fragmentation [80–84]. Assessing the equivalent bare charge mass is a common method to address this reduction in blast power. The nature of combined loading, considering these effects, is complex and exhibits a synergistic effect, causing more severe damage and structural response than detonation without a casing. Design guidelines often oversimplify or neglect these combined effects, potentially leading to nonconservative designs. Experimental, analytical, and numerical studies [85–87] have comprehensively investigated the combined loading effect. They developed methods to assess fragmentation impulses and validated them through tests and simulations, highlighting the importance of considering fragmentation impulses in design. Experimental studies on RC T-walls subjected to detonations [85] demonstrated significant damage inflicted by fragments, underscoring the necessity of accounting for fragment effects in structural design and analysis. Advanced models have been developed to assess dynamic responses to combined blast and fragment loading.

Modelling the combined effects of explosions and fragment projections on reinforced concrete protective structures poses a significant challenge due to their highly dynamic and nonlinear behaviour.

A conservative approach involves assessing the reduced bare charge due to diminished blast intensity from a cased charge and evaluating blast and fragment impulses. However, fragmentation impulses are often overlooked.

It is crucial to recognize that an RC element realistic response to combined blast and fragment loading involves a coupled problem, particularly at closer distances. However, decoupling effects become more accurate at greater distances, where fragments impact the structure before the blast.

The most commonly used formulas for the assessment of the equivalent bare charge mass are the Fisher and Fano formulas [88]. These methods are based on energy considerations and further assumptions regarding energy loss in the detonation process. However, Hutchinson [82] claimed that these formulas are not accurate, indicating inaccuracies in their assumptions. He developed a new, more physically based formula. For low M/C ratios, where M is the casing mass and C is the charge mass, the results are similar to those of the Fisher and Fano formulas, but for very large M/C ratios, the M/C ratio converges to zero, which is physically expected.

Although the prediction of blast pressures is more trivial and there are various methods for this prediction (experimental studies, numerical simulations, or empirically based diagrams), methods for assessing fragmentation impulses are rare. Grisaro and Dancygier [89] proposed a method for accessing common cylindrical shaped charges.

When the impulse of the fragments is significant compared to the blast impulse, damage due to the penetration of the fragments should also be considered. A simplified approach to this task is to consider an effectively reduced cross-sectional height of the damaged structural element; this reduction is relevant mainly for small standoff distances. Grisaro and Dancygier [87] presented a method to assess this reduction based on an experimental study.

More detailed modelling of the combined effects of explosions and fragment projections on reinforced concrete protective structures poses significant challenges due to the highly dynamic and nonlinear nature of such events. To address this complexity, current methodologies typically employ a multistep approach [90], as outlined below:

(1) Simulating blast loading and structural response: this involves using a coupled model that integrates simplified concrete models to account for pressure wave reflections and the failure of concrete, facilitating the venting of blast pressure. Computational fluid dynamics software, such as LS-Dyna or Autodyn, is utilized to determine the blast pressure. The process involves fine Eulerian discretization to simulate detonation and casing break-up, with cell merging employed further away from the blast source. A bilinear pressure–time curve is derived from the blast impulse, with one segment representing the initial high-pressure peak and another considering wave reflections. The gas pressure is determined from this curve, considering the casing mass.
(2) Fragment loading analysis: this step involves defining characteristics such as fragment mass, launch angle, and velocity. It is assumed that fragments are generated by the failure of casing projectiles. The collisions between fragments are considered, assuming an inelastic collision model where mass and momentum are conserved. The fragment penetration depth and impact velocity are determined empirically, with the pressure on the structure calculated based on these factors.
(3) Advanced FE analysis: advanced FE tools such as LS-Dyna or Autodyn are employed to model the detailed structural behaviour under blast and fragment loading. Pressure–time curves obtained from the blast and impact analyses are applied to the model. Structural erosion is simulated by defining areas of constant pressure on meshed shell elements, facilitating a more accurate representation of the structural response.

4.4 Combined effects of explosions and fire

The combined effect of explosion and fire includes both situations where the explosion is the extreme consequence of a fire and situations where a blast is also followed by a fire. A classic example of the first situation is the accidental scenario of a serious collision of vehicles in a tunnel, which initially develops a fire and then results in an explosion. An example of the second situation is the gas explosion in a building, which is followed by a fire provoked by the explosion. Compared to studies analysing the behaviour of concrete structures subjected to explosions, experimental and numerical studies (even simplified ones) on reinforced concrete structures exposed to the combined effects of fire and blast are much more limited [91–97].

The effect due to the fire must be added to the methods of different complexities described in Sect. 4.1 to consider the explosion. In both cases of blast-fire interaction, the approach may involve either a) coupled thermo-mechanical analysis or b) decoupling the phenomena and sequentially treating the effects due to the explosion and the effects due to the fire in the desired sequence. For example, in case b), if a fire precedes an explosion, the fire effects can be initially considered in a simplified way by adopting temperature-dependent mechanical material properties and defining, for the cross section, a generalized constitutive law (i.e., moment–curvature diagram) that accounts for fire effects and that can be used for a subsequent mechanical analysis that accounts for a blast. This approach is used in [93] for analysing underground tunnels subjected to internal explosions preceded by fire actions.

When fire exposure follows the blast load, the design approaches previously described for the blast situation alone can be adopted to fix the damage level of the structure after the blast, and a traditional fire design approach (which is not the object of this document) can be adopted for a pre-damaged structure.

It is worth noting that all the considerations related to the blast load presented in the previous paragraphs remain valid even in this case.

When a fire precedes a blast, different types of analyses can be used. A list of possible types is reported below:

(1) Linear SDOF system reduction.
(2) Linear elastic FE analysis with beam elements.
(3) Nonlinear SDOF system reduction.
(4) Nonlinear FE analysis with beam elements.
(5) Coupled thermo-mechanical nonlinear FE analysis with 3D elements.

In Colombo and Martinelli [98], approaches (1) to (4) for constructing pressure–impulse diagrams of reinforced concrete structures subjected to both a blast and a blast preceded by fire are compared. Using a statically indeterminate beam with three supports as the reference case, their work examined the influence of various analysis methods (analytical approach with an elastic shape function, linear elastic FE analysis, analytical approach with a plastic shape function, and nonlinear FE analysis) on the safety level, as assessed through pressure–impulse diagrams.

Methods 1–4 decouple the fire and explosion phenomena and are commonly used in design practice, while method 5 represents the most sophisticated method, allowing the definition of material properties as a function of temperature and strain rate. However, the adoption of this method is limited by the complexity and size of the model, as well as the need for accurate parameters to characterize material behaviour.

It is important to point out that often in the case of blasts, the dynamic effect can lead to different failure mechanisms with respect to those expected under static conditions. Methods 1 and 3 define the structural behaviour from which the failure mechanism ensues a priori and are not able to predict any variation in the failure mechanism with increasing strain rate. Method 2, even if it can provide a computation of the strain rate, is related to the elastic behaviour of the structure and not to the real nonlinear response. Method 4 can consider the strain rate effect (depending on the element formulation), but the failure criteria and mechanism are always strictly related to the element formulation and integration. Finally, method 5 is the only method that can automatically consider the strain rate effect and can predict the change in the failure mechanism due to the strain rate effect.

5 Evaluation of the initial and residual bearing capacities of the structure

Concrete structures, including offshore platforms, nuclear power plants, and highway bridges, are frequently exposed to intense but short-lived loads during their operational lifespan, such as impacts, explosions, or seismic events. Therefore, it is crucial to comprehend how concrete and concrete structures behave under dynamic loading conditions to establish safety margins and develop reliable yet cost-effective design procedures, because the loading rate can simultaneously affect the resistance, failure mode, crack pattern and propagation velocity [14, 15, 19, 23–26].

Modern numerical modelling techniques, such as finite element methods employing discrete or smeared crack models, adaptive discretization strategies, and advanced contact formulations, enable detailed investigations of complex three-dimensional dynamic fractures in concrete structures. However, the success of these simulations hinges on the adequacy of the constitutive equation in capturing the macroscopic material behaviour under dynamic conditions.

As already discussed, the behaviour of concrete materials under dynamic loading is significantly influenced by the loading rate. This rate-dependent response is governed by three primary effects: the rate dependence of microcrack growth, the viscous behaviour of the material between cracks, and various forms of inertia. While the first two effects can be addressed through macro- or meso-level analysis using rate-dependent constitutive laws, the third effect can be automatically accounted for in dynamic analyses where the constitutive law interacts with inertial forces and the mesh is fine enough [23–26, 28]. Note that the effectiveness in covering the third aspect differs per material model. Plasticity and damage models appear to be less effective than the micro-plane model (see Sect. 3.5).

The dominance of these effects varies depending on factors such as material type, structure, and loading rate. For concrete and similar quasi-brittle materials, microcrack growth and viscosity play significant roles at lower to medium loading rates, while inertia becomes predominant at higher rates, such as during impact events. At a certain threshold loading rate, inertia leads to a progressive increase in resistance and a shift in failure modes, such as from bending to shear failure [28, 80, 99].

As the loading rate increases, the failure mode tends to transition from mode I to mixed modes due to the homogenizing effect of inertia in the impact zone. Crack propagation under dynamic loading may be impeded by inertia, leading to crack branching and complex failure patterns. This effect is particularly pronounced in quasi-brittle materials such as concrete and ductile materials such as steel, where inertia significantly influences resistance and ductility.

Designing concrete structures (with different reinforcements) under blast or impact loading requires careful consideration of the dynamic failure mechanisms and their effects on structural integrity. Unlike quasi-static loading, where cross-sectional analysis suffices, dynamic loading necessitates examining each structural element individually to assess its residual strength post-event. Pressure–impulse curves can be established based on experimental or numerical investigations to inform design decisions and ensure structural resilience.

In scenarios where the influence of inertia on the failure mode and resistance is minimal, cross-sectional analyses such as quasi-static loading may still be applicable. This typically occurs at lower loading rates or for smaller structural elements where failure modes remain consistent, allowing for the application of dynamic increase factors on material strength. Structural elements exhibiting shear failure at higher loading rates may also maintain consistent failure modes, enabling the use of rate-dependent constitutive laws to approximate resistance increases.

6 Structural design strategies for protective structures

While this report is applicable to any type of concrete structure, this section focuses on design strategies for protective structures. Protective structures are essential for safeguarding against various extreme loads, including blasts, impacts, or a combination of both [82, 89, 100]. These structures serve diverse purposes, ranging from military installations to civil structures such as shelters, nuclear containment buildings, or rock sheds. Understanding the types of loads and threats they face is crucial for designing effective protective measures.

Extreme loads can arise from accidents such as vehicle collisions or airplane crashes, as well as deliberate acts of terrorism or military attacks involving blasts and fragmentation. Blast overpressure can also occur accidentally, such as from explosions of hazardous materials, for example, gas [101]. Differentiating between accidental and deliberate loads helps in designing appropriate protection measures.

Assessing resistance to extreme loads involves both structural failure criteria and measures specific to impact resistance. Structural failure criteria consider global responses such as flexural or shear failure modes, while impact-specific measures focus on phenomena such as perforation and front and rear face damage. The quantification of resistance involves parameters such as the penetration depth, front and rear face damage, and ballistic limits (in the case of perforation).

Reinforced concrete is commonly used in protective barriers due to its massiveness and cost-effectiveness. The thickness of RC structures should be considered to prevent perforation and rear face scabbing. However, the influence of conventional steel reinforcement on impact resistance remains debated, with studies suggesting various effects on penetration depth and damage [102, 103].

High-strength concrete (HSC) offers increased resistance to penetration, but its brittleness can lead to greater damage at the rear face of impacted barriers [102–111]. Concrete mix ingredients, including aggregate size [112–115] and hardness [116, 117], play crucial roles in enhancing resistance while minimizing damage. The effectiveness of HSC in reducing penetration depth and front face craters is evident from the experimental results. Rebentrost and Wight [118] conducted large-scale blast tests, close-charge blast tests, fragment simulation tests, and ballistic tests, demonstrating that UHPC panels optimized for blast resistance are an effective solution for infrastructure protection. These panels exhibit exceptional energy absorption capacity and resistance to fragmentation.

Steel fibre-reinforced concrete also enhances impact resistance by minimizing damaged areas and reducing penetration depth [112, 113, 115–122].

Structural design strategies such as external protective layers [123–126], double-layer cross-sections

[127], and confinement techniques [128] further enhance the performance of protective barriers.

Reinforcement can provide confinement to increase concrete strength and deformation capacities, thereby enhancing resistance to penetration and perforation. Limited studies on the response of confined concrete to impact have shown promising results, suggesting reduced damage and improved resistance. However, implementing confinement in protective barrier design warrants further investigation.

7 Conclusions

The article offers a state-of-the-art review of research endeavours and current design guidelines regarding the structural response of concrete structures to impact and blast loads: design strategies tailored for concrete construction under extreme loading conditions are presented. The high strain rate behaviour of materials is discussed; various analysis methods employed for explosion, impact, combined explosions and fragments, as well as the combined effects of explosions and fire are outlined. Additionally, this study provides a brief overview of evaluating both the initial and residual bearing capacity of concrete structures. Finally, the structural design strategies for concrete protective barriers are also examined.

Acknowledgements The authors gratefully acknowledge the contributions of all TC members to the discussions held during the preparation of this report. Special thanks are extended to Prof. Gonzalo Ruiz for his valuable comments, which improved the manuscript. The authors also wish to express their deep appreciation to Dr. Alessio Caverzan for his substantial contribution to the development of this report.

Funding Open access funding provided by Politecnico di Milano within the CRUI-CARE Agreement.

Open Access This article is licensed under a Creative Commons Attribution 4.0 International License, which permits use, sharing, adaptation, distribution and reproduction in any medium or format, as long as you give appropriate credit to the original author(s) and the source, provide a link to the Creative Commons licence, and indicate if changes were made. The images or other third party material in this article are included in the article's Creative Commons licence, unless indicated otherwise in a credit line to the material. If material is not included in the article's Creative Commons licence and your intended use is not permitted by statutory regulation or exceeds the permitted use, you will need to obtain permission directly from the copyright holder. To view a copy of this licence, visit http://creativecommons.org/licenses/by/4.0/.

References

1. Technical Committee RILEM-IEC. (2020). Report on Experimental Devices Harvest for Impact and Explosion Testing of Materials and Structures. Retrieved from https://www.rilem.net/global/gene/link.php?news_link=2020153210_report-iec-def1-ec1.pdf&fg=1
2. Fédération internationale du béton (fib). (2023). fib Model Code for Concrete Structures (2020). 780 pages. ISBN: 978–2–88394–175–5.
3. Baker WE, Cox PA, Westine PS, Kulesz JJ, Strehlow RA (1983) Explosion Hazards and Evaluation. Elsevier Scientific Publishing Company, Amsterdam-Oxford-New York
4. Krauthammer T (2008) Modern protective structures. CRC Press, Boca Raton. https://doi.org/10.1201/9781420015423
5. Van den Berg AC (1985) The multi-energy method: a framework for vapour cloud explosion blast prediction. J Hazard Mater 12(1):1–10. https://doi.org/10.1016/0304-3894(85)80022-4
6. Van den Berg AC (2009) "BLAST": a compilation of codes for the numerical simulation of the gas dynamics of explosions. J Loss Prev Process Ind 22(3):271–278. https://doi.org/10.1016/j.jlp.2008.07.004
7. CEN (2006) EN 1991-1-7: Eurocode 1—Actions on structures—Part 1–7: General actions—Accidental actions. Belgium, Brussels
8. Fédération internationale du béton (fib). (2012). fib Bulletin 63: Design of precast concrete structures against accidental actions. 78 pages. ISBN 978–2–88394–103–8
9. Biggs J (1964) Introduction to structural dynamics. McGraw-Hill Book Company, New York
10. Clough RW, Penzien J (1993) Dynamics of structures, 2nd edn. McGraw Hill, New York
11. Humar JL (2002) Dynamics of structures. Balkema Publishers, Exton, PA
12. Freund LB (1972) Crack propagation in an elastic solid subjected to general loading-I. Constant rate of extension. J Mech Phys Solids 20(3):129–140. https://doi.org/10.1016/0022-5096(72)90006-3
13. Freund LB (1972) Crack propagation in an elastic solid subjected to general loading-II. Non-uniform rate of extension. J Mech Phys Solids 20(3):141–152. https://doi.org/10.1016/0022-5096(72)90007-5
14. Reinhardt HW (1982) Concrete under impact loading, tensile strength and bond. Heron 27(3):1–48
15. Dilger WH, Koch R, Kowalczyk R (1984) Ductility of plain and confined concrete under different strain rates. Am Concr Inst 81(1):73–81. https://doi.org/10.14359/10649
16. Banthia NP, Mindess S, Bentur A (1987) Impact behaviour of concrete beams. Mater Struct/Matériaux et Constructions 20:293–302. https://doi.org/10.1007/BF02485926

17. Bischoff P, Perry S (1991) Compressive behaviour of concrete at high strain rates. Mater Struct/Matériaux et Constructions 24:425–450. https://doi.org/10.1007/BF024720
18. Reinhardt HW, Weerheijm J (1991) Tensile fracture of concrete at high loading rates taking account of inertia and crack velocity effects. Int J Fract 51:31–42. https://doi.org/10.1007/BF00020851
19. Weerheijm, J. (1992). Concrete under impact tensile loading and lateral compression. Dissertation, TU Delft, The Netherlands.
20. Larcher M (2009) Development of discrete cracks in concrete loaded by shock waves. Int J Impact Eng 36(5):700–710. https://doi.org/10.1016/j.ijimpeng.2008.10.003
21. Pedersen RR (2009) Computational modelling of dynamic failure of cementitious materials. Dissertation, TU Delft, the Netherlands.
22. International Federation for Structural Concrete (fib) (2013). fib Model Code for Concrete Structures 2010. https://doi.org/10.1002/9783433604090.
23. Mu ZC, Dancygier AN, Zhang W, Yankelevsky DZ (2012) Revisiting the dynamic compressive behavior of concrete-like materials. Int J Impact Eng 49:91–102. https://doi.org/10.1016/j.ijimpeng.2012.05.002
24. Ožbolt J, Bošnjak J, Sola E (2013) Dynamic fracture of concrete compact tension specimen: experimental and numerical study. Int J Solids Struct 50(25–26):4270–4278. https://doi.org/10.1016/j.ijsolstr.2013.08.030
25. Ožbolt J, Bede N, Sharma A, Mayer U (2015) Dynamic fracture of concrete L-specimen: experimental and numerical study. Eng Fract Mech 148:27–41. https://doi.org/10.1016/j.engfracmech.2015.09.002
26. Gambarelli S, Ožbolt J (2020) Dynamic fracture of concrete in compression: 3D finite element analysis at meso- and macro-scale. Continuum Mech Thermodyn 32:1803–1821. https://doi.org/10.1007/s00161-020-00881-5
27. Ožbolt J, Rah KK, Mestrovic D (2006) Influence of loading rate on concrete cone failure. Int J Fract 139:239–252. https://doi.org/10.1007/s10704-006-0041-3
28. Ožbolt J, Sharma A, Reinhardt HW (2011) Dynamic fracture of concrete—compact tension specimen. Int J Solid Struct 48(10):1534–1543. https://doi.org/10.1016/j.ijsolstr.2011.01.033
29. Department of Defense (DoD) (2009) UFC 4–023-03: Design of buildings to resist progressive collapse. DC (US), Washington
30. Riedel W, Forquin P (2024) Dynamic response regimes of concrete structures. In: Weerheijm J (Ed.), Understanding the Tensile Properties of Concrete (Second Edition) (pp. 117–131). Woodhead Publishing Series in Civil and Structural Engineering. Woodhead Publishing. ISBN: 9780443155932. https://doi.org/10.1016/B978-0-443-15593-2.00013-0
31. Hentz S, Donzé FV, Daudeville L (2004) Discrete element modelling of concrete submitted to dynamic loading at high strain rates. Comput Struct 82(29–30):2509–2524. https://doi.org/10.1016/j.compstruc.2004.05.016
32. Gilat A, Schmidt TE, Walker AL (2009) Full field strain measurement in compression and tensile split hopkinson bar experiments. Exp Mech 49:291–302. https://doi.org/10.1007/s11340-008-9157-x
33. Cadoni E, Dotta M, Forni D, Tesio N, Albertini C (2013) Mechanical behaviour of quenched and self-tempered reinforcing steel in tension under high strain rate. Mater Des 49:657–666. https://doi.org/10.1016/j.matdes.2013.02.008
34. Cadoni E, Dotta M, Forni D, Tesio N (2015) High strain rate behaviour in tension of steel B500A reinforcing bar. Mater Struct 48(6):1803–1813. https://doi.org/10.1617/s11527-014-0273-z
35. Clausen AH (2018) Tensile testing using the kolsky-hopkinson bar machine. In: Othman, R. (eds) The Kolsky-Hopkinson Bar Machine. Springer, Cham. https://doi.org/10.1007/978-3-319-71919-1_2.
36. ACI Sub-committee 544–0E (2018). FRC-Emerging Technologies. American Concrete Institute, Farmington Hills, MI.
37. Toutlemonde F, Gary G (2009) Dynamic behavior of concrete: experimental aspects. In: Mazars J, Millard A (Eds.), Dynamic behavior of concrete and seismic engineering (pp 1–54). https://doi.org/10.1002/9780470611555.ch1
38. Forquin, P., Riedel, W., & Weerheijm, J. (2024). Dynamic testing devices. In J. Weerheijm (Ed.), Understanding the Tensile Properties of Concrete (Second Edition) (pp. 133–175). Woodhead Publishing Series in Civil and Structural Engineering. Woodhead Publishing. ISBN: 9780443155932. https://doi.org/10.1016/B978-0-443-15593-2.00002-6
39. Pajak M, Baranowski P, Janiszewski J, Kucewicz M, Mazurkiewicz L, Lazniewska-Piekarczyk B (2021) Experimental testing and 3D meso-scale numerical simulations of SCC subjected to high compression strain rates. Constr Build Mater 302:124379. https://doi.org/10.1016/j.conbuildmat.2021.124379
40. Guo YB, Gao GF, Jing L, Shim VPW (2017) Response of high-strength concrete to dynamic compressive loading. Int J Impact Eng 108:114–135. https://doi.org/10.1016/j.ijimpeng.2017.04.015
41. Wang Y, Wang Z, Liang X, An M (2008) Experimental and numerical studies on dynamic compressive behavior of reactive powder concretes. Acta Mech Solida Sin 21(5):420–430. https://doi.org/10.1007/s10338-008-0851-0
42. Hou X, Cao S, Zheng W, Rong Q, Li G (2018) Experimental study on dynamic compressive properties of fiber-reinforced reactive powder concrete at high strain rates. Eng Struct 169:119–130. https://doi.org/10.1016/j.engstruct.2018.05.036
43. Ren GM, Wu H, Fang Q, Liu JZ (2018) Effects of steel fiber content and type on dynamic compressive mechanical properties of UHPCC. Constr Build Mater 164:29–43. https://doi.org/10.1016/j.conbuildmat.2017.12.203
44. Cadoni E, Forni D, Bonnet E, Dobrusky S (2019) Experimental study on direct tensile behaviour of UHPFRC under high strain-rates. Constr Build Mater 218:667–680. https://doi.org/10.1016/j.conbuildmat.2019.05.152
45. Pajak M, Janiszewski J, Kruszka L (2019) Laboratory investigation on the influence of high compressive strain rates on the hybrid fibre reinforced self-compacting

concrete. Constr Build Mater 227:116687. https://doi.org/10.1016/j.conbuildmat.2019.116687
46. Malvar LJ (1998) Review of static and dynamic properties of steel reinforcing bars. ACI Mater J 95(5):609–616. https://doi.org/10.14359/403
47. Cadoni E, Fenu L, Forni D (2012) Strain rate behaviour in tension of austenitic stainless steel used for reinforcing bars. Constr Build Mater 35:399–407. https://doi.org/10.1016/j.conbuildmat.2012.04.081
48. Cadoni E, Fontana M, Forni D, Knobloch M (2018) High strain rates testing and constitutive modeling of B500B reinforcing steel at elevated temperatures. Eur Phys J Spec Top 227:179–199. https://doi.org/10.1140/epjst/e2018-00046-4
49. Cadoni E, Forni D (2019) Austenitic stainless steel under extreme combined conditions of loading and temperature. J Dyn Behav Mater 5:230–240. https://doi.org/10.1007/s40870-019-00205-y
50. Cadoni E, Forni D (2021) Mechanical behaviour of B500A rebars: effect of elevated temperature and high strain-rate. Fire Saf J 122:103321. https://doi.org/10.1016/j.firesaf.2021.103321
51. Ožbolt J, Sharma A, Irhan B, Sola E (2014) Tensile behavior of concrete under high loading rates. Int J Impact Eng 69:55–68. https://doi.org/10.1016/j.ijimpeng.2014.02.005
52. Abrams DA (1917) Effect of rate of application of load on the compressive strength of concrete. ASTM J 17:364–377
53. Evans RH (1942) Effect of rate of loading on the mechanical properties of some materials. J Inst Civ Eng 48(7):296–306. https://doi.org/10.1680/ijoti.1942.13813
54. Hughes BP, Watson AJ (1978) Compressive strength and ultimate strain of concrete under impact loading. Mag Concr Res 30(105):189–199. https://doi.org/10.1680/macr.1978.30.105.189
55. Malvern LE, Ross CA (1985) Dynamic response of concrete and concrete structures. Second Annual Technical Report. AFOSR Contract No. F49620–83-K007.
56. Ross CA, Thompson PY, Tedesco JW (1989) Split-Hopkinson pressure-bar tests on concrete and mortar in tension and compression. ACI Mater J 86(5):475–481. https://doi.org/10.14359/2065
57. Ross CA, Tedesco JW, Kuennen ST (1995) Effects of strain rate on concrete strength. ACI Mater J 92(1):37–47. https://doi.org/10.14359/1175
58. Tedesco JW, Ross CA (1998) Strain-rate-dependent constitutive equations for concrete. ASME J Press Vessel Technol 120(4):398–405. https://doi.org/10.1115/1.2842350
59. Grote DL, Park SW, Zhou M (2001) Dynamic behavior of concrete at high strain rates and pressures: I. Experimental characterization. Int J Impact Eng 25(9):869–886. https://doi.org/10.1016/S0734-743X(01)00020-3
60. Hao Y, Hao H, Jiang GP, Zhou Y (2013) Experimental confirmation of some factors influencing dynamic concrete compressive strengths in high-speed impact tests. Cem Concr Res 52:63–70. https://doi.org/10.1016/j.cemconres.2013.05.008
61. Chen X, Wu S, Zhou J (2013) Experimental and modeling study of dynamic mechanical properties of cement paste, mortar and concrete. Constr Build Mater 47:419–430. https://doi.org/10.1016/j.conbuildmat.2013.05.063
62. Salloum YA, Almusallam T, Ibrahim SM, Abbas H, Alsayed S (2015) Rate dependent behavior and modeling of concrete based on SHPB. Cement Concr Compos 55:34–44. https://doi.org/10.1016/j.cemconcomp.2014.07.011
63. Comite Euro-International du Beton (1993) CEB-FIP model code 1990. Redwood Books, Trowbridge, Wiltshire, UK
64. Li QM, Meng H (2003) About the dynamic strength enhancement of concrete-like materials in a split Hopkinson pressure bar test. Int J Solids Struct 40(2):343–360. https://doi.org/10.1016/S0020-7683(02)00526-7
65. Hao Y, Hao H, Li ZX (2013) Influence of end friction confinement on impact tests of concrete material at high strain rate. Int J Impact Eng 60:82–106. https://doi.org/10.1016/j.ijimpeng.2013.04.008
66. Hao H, Hao Y, Li J, Chen W (2016) Review of the current practices in blast-resistant analysis and design of concrete structures. Adv Struct Eng 19(8):1193–1223. https://doi.org/10.1177/1369433216656430
67. Weerheijm J et al (2024) Understanding the tensile properties of concrete: In: Statics and Dynamics. 2nd edition. Woodhead publishing series in civil and structural engineering. Elsevier. ISBN: 978–0–443–15594–2
68. Sharma A, Ožbolt J (2014) Influence of high loading rates on behavior of reinforced concrete beams with different aspect ratios–a numerical study. Eng Struct 79:297–308. https://doi.org/10.1016/j.engstruct.2014.08.025
69. U.S. Department of Defense (DoD). (2008). Unified facilities criteria (UFC)—Structures to resist the effects of accidental explosions (UFC 3–340–02).
70. Hallquist J (2006) LS-Dyna theory manual. Livermore software technology corporation, Livermore, California
71. Gexcon AS. (2021). FLACS-CFD 21.2 User Manual. Bergen, Norway: Gexcon AS.
72. Fraunhofer Ernst Mach Institute. (2018). APOLLO Blastsimulator manual, version: 2018.2. Freiburg, Germany: Fraunhofer EMI.
73. Krauthammer T, Astarlioglu S, Blasko J, Soh TB, Ng PH (2008) Pressure-impulse diagrams for the behavior assessment of structural components. Int J Impact Eng 35:771–783
74. Colombo M, Martinelli P (2012) Pressure-impulse diagrams for RC and FRC circular plates under blast loads. Eur J Environ Civ Eng 16(7):837–862. https://doi.org/10.1080/19648189.2012.675149
75. Abedini M, Mutalib AA, Raman SN, Alipour R, Akhlaghi E (2019) Pressure-Impulse (P–I) diagrams for Reinforced Concrete (RC) structures: a review. Arch Comput Methods Eng 26:733–767. https://doi.org/10.1007/s11831-018-9260-9
76. CEB Bulletin n. 187 (1988). Concrete structures under impact and impulsive loading—synthesis report. Lausanne, 184 pages.
77. Yankelevsky D (1982) Interaction of soil and penetrating projectile. J Geotech Div, ASCE J Geotech Eng Div 108(3):493–497. https://doi.org/10.1061/AJGEB6.0001263

78. Irhan B, Ožbolt J, Ruta D (2015) 3D finite element simulations of high velocity projectile impact. Int J Solids Struct 72:38–49. https://doi.org/10.1016/j.ijsolstr.2015.07.010
79. Leppänen J (2004) Concrete structures subjected to fragment impacts. Doctoral Thesis, Chalmers University of Technology
80. Nystrom UGK (2009) Numerical studies of the combined effects of blast and fragment loading. Int J Impact Eng 36(8):995–1005. https://doi.org/10.1016/j.ijimpeng.2009.02.008
81. Grisaro H, Dancygier AN (2016) On the problem of bare-to-cased charge equivalency. Int J Impact Eng 94:13–22. https://doi.org/10.1016/j.ijimpeng.2016.03.004
82. Hutchinson MD (2009) The escape of blast from fragmenting munitions casings. Int J Impact Eng 36(2):185–192. https://doi.org/10.1016/j.ijimpeng.2008.05.002
83. Leppänen J (2005) Experiments and numerical analyses of blast and fragment impacts on concrete. Int J Impact Eng 31(7):843–860. https://doi.org/10.1016/j.ijimpeng.2004.04.012
84. Mcvay MK (1988) Spall damage of concrete structures. Technical report SL-88–22, Structures Laboratory, Department of the Army, Waterways Experiment Station, Corps of Engineers, Vicksburg, Mississippi, USA
85. Grisaro HY, Benamou D, Dancygier AN (2018) Investigation of blast and fragmentation loading characteristics—field tests. Eng Struct 167:363–375. https://doi.org/10.1016/j.engstruct.2018.04.013
86. Grisaro HY, Dancygier AN, Benamou D (2019) Structural properties of RC plates damaged by fragmentation impact. Constr Build Mater 207:463–476. https://doi.org/10.1016/j.conbuildmat.2019.02.096
87. Grisaro HY, Dancygier AN (2019) Representation of damage caused by fragmentation impact in design and analysis of reinforced concrete barriers. Eng Struct 197:109387. https://doi.org/10.1016/j.engstruct.2019.109387
88. Fischer EM (1953) The effect of the steel case on the air blast. Report 2753, Naval Ordnance Laboratory, White Oak, MD, USA
89. Grisaro HY, Dancygier AN (2018) Characteristics of combined blast and fragments loading. Int J Impact Eng 116:51–64. https://doi.org/10.1016/j.ijimpeng.2018.02.004
90. Weerheijm J, Stolz A, Riedel W, Mediavilla J (2012) Modelling loading and break-up of RC Structure due to internal explosion of fragmenting shells. In: MABS22: 22nd International Symposium on Military Aspects of Blast and Shock. Bourges, France
91. Kakogiannis D, Pascualena F, Reymen B, Pyl L, Ndambi JM, Segers E et al (2013) Blast performance of reinforced concrete hollow core slabs in combination with fire: numerical and experimental assessment. Fire Saf J 57:69–82. https://doi.org/10.1016/j.firesaf.2012.10.027
92. Ruan Z, Chen L, Fang Q (2015) Numerical investigation into dynamic responses of RC columns subjected for fire and blast. J Loss Prev Process Ind 34:10–21. https://doi.org/10.1016/j.jlp.2015.01.009
93. Colombo M, Martinelli P, di Prisco M (2015) A design approach for tunnels exposed to blast and fire. Struct Concr 16(2):262–272. https://doi.org/10.1002/suco.201400052
94. Zhai C, Chen L, Xiang H, Fang Q (2016) Experimental and numerical investigation into RC beams subjected to blast after exposure to fire. Int J Impact Eng 97:29–45. https://doi.org/10.1016/j.ijimpeng.2016.06.004
95. Pan L, Chen L, Fang Q, Zhai C, Pan T (2016) A modified layered-section method for responses of fire-damaged reinforced concrete beams under static and blast loads. Int J Prot Struct 7(4):495–517. https://doi.org/10.1177/2041419616658384
96. Roy T, Matsagar V (2021) Mechanics of damage in reinforced concrete member under post-blast fire scenario. Structures 31:740–760. https://doi.org/10.1016/j.istruc.2021.02.005
97. Colombo M, Martinelli P, Arano A, Øverli JA, Hendriks MAN, Kanstad T, di Prisco M (2021) Experimental investigation on the structural response of RC slabs subjected to combined fire and blast. Structures 31:1017–1030. https://doi.org/10.1016/j.istruc.2021.02.029
98. Colombo M, Martinelli P (2024) Pressure–impulse diagrams of RC beams considering fire–blast interaction. Struct Concr. https://doi.org/10.1002/suco.202300513
99. Ožbolt J, Tonkovic Z, Lackovic L (2016) Microplane model for steel and application on static and dynamic fracture. J Eng Mech, ASCE 142(2):04015086. https://doi.org/10.1061/(ASCE)EM.1943-7889.0000993
100. Marchand KA, Vargas MM, Nixon JD (1992) The synergistic effects of combined blast and fragment loading. San Antonio, Texas: Southwest Research Institute; 1992. Report ESL-TR-91–18
101. Pearson C, Delatte N (2005) Ronan point apartment tower collapse and its effect on building codes. ASCE J Perform Constr Facil 19(2):172–177. https://doi.org/10.1061/(ASCE)0887-3828(2005)19:2(172)
102. Kennedy RP (1976) A review of procedures for the analysis and design of concrete structures to resist missile impact effects. Nucl Eng Des 37(2):183–203. https://doi.org/10.1016/0029-5493(76)90015-7
103. Li QM, Reid SR, Wen HM, Telford AR (2005) Local impact effects of hard missiles on concrete targets. Int J Impact Eng 32(1–4):224–284. https://doi.org/10.1016/j.ijimpeng.2005.04.005
104. NDRC (1946) Effects of impact and explosion. Summary technical report of division 2, National Defense Research Committee (NDRC), vol. 1, Washington D.C.
105. Forrestal MJ, Altman BS, Cargile JD, Hanchak SJ (1994) An empirical depth of penetration equation for penetration ogive-nose projectiles concrete targets. Int J Impact Eng 15(4):395–405. https://doi.org/10.1016/0734-743X(94)80024-4
106. Sliter GE (1980) Assessment of empirical concrete impact formulas. J Struct Div, ASCE 106(5):1023–1045. https://doi.org/10.1061/JSDEAG.0005413
107. Berriaud C, Sokolovsky A, Gueraud R, Dulac J, Labrot R (1978) Local behaviour of reinforced concrete walls under missile impact. Nucl Eng Des 45:457–469. https://doi.org/10.1016/0029-5493(78)90235-2

108. Haldar A, Hamieh H (1984) Local effect of solid missiles on concrete structures. ASCE J Struct Div 110(5):948–960. https://doi.org/10.1061/(ASCE)0733-9445(1984)110:5(948)
109. Hughes G (1984) Hard missile impact on reinforced concrete. Nucl Eng Des 77(1):23–35. https://doi.org/10.1016/0029-5493(84)90058-X
110. Barr P (1990) Guidelines for the design and assessment of concrete structures subjected to impact. Report, UK Atomic Energy Authority, Safety and Reliability Directorate, HMSO, London
111. Williams MS (1994) Modeling of local impact effects on plain and reinforced concrete. ACI Struct J 91(2):178–187. https://doi.org/10.14359/4603
112. Zhang MH, Shim VPW, Lu G, Chew CW (2005) Resistance of high-strength concrete to projectile impact. Int J Impact Eng 31(7):825–841. https://doi.org/10.1016/j.ijimpeng.2004.04.009
113. Dancygier AN, Yankelevsky DZ, Jaegermann C (2007) Response of high performance concrete plates to impact of non-deforming projectiles. Int J Impact Eng 34(11):1768–1779. https://doi.org/10.1016/j.ijimpeng.2006.09.094
114. Bludau C, Keuser M, Kustermann A (2006) Perforation resistance of high-strength concrete panels. ACI Struct J 103(2):188–195. https://doi.org/10.14359/15176
115. Werner S, Thienel KC, Kustermann A (2013) Study of fractured surfaces of concrete caused by projectile impact. Int J Impact Eng 52:23–27. https://doi.org/10.1016/j.ijimpeng.2012.09.005
116. Frew DJ, Hanchak SJ, Green ML (1998) Penetration of concrete targets with ogive nose steel rods. Int J Impact Eng 21(6):489–497. https://doi.org/10.1016/S0734-743X(98)00008-6
117. Forrestal MJ, Frew DJ, Hanchak SJ, Brar NS (1996) Penetration of grout and concrete targets with ogive-nose steel projectiles. Int J Impact Eng 18(5):465–476. https://doi.org/10.1016/0734-743X(95)00048-F
118. Rebentrost M, Wight G (2013) Investigation of UHPFRC slabs under blast loads. In: Designing and Building with UHPFRC (pp. 363–376). https://doi.org/10.1002/9781118557839.ch24
119. Almusallam TH, Siddiqui NA, Iqbal RA, Abbas H (2013) Response of hybrid-fiber reinforced concrete slabs to hard projectile impact. Int J Impact Eng 58:17–30. https://doi.org/10.1016/j.ijimpeng.2013.02.005
120. Almusallam TH, Abadel AA, Al-Salloum YA, Siddiqui NA, Abbas H (2015) Effectiveness of hybrid-fibers in improving the impact resistance of RC slabs. Int J Impact Eng 81:61–73. https://doi.org/10.1016/j.ijimpeng.2015.03.010
121. Almansa EM, Canovas MF (1999) Behavior of normal and steel fibers-reinforced concrete under impact of small projectiles. Cem Concr Res 29(11):1807–1814. https://doi.org/10.1016/S0008-8846(99)00174-X
122. Ong KCG, Basheerkhan M, Paramasivam P (1999) Resistance of fibre concrete slabs to low velocity projectile impact. Cement Concr Compos 21(5–6):391–401. https://doi.org/10.1016/S0958-9465(99)00024-4
123. Barr P, Carter PG, Howe WD, Neilson AJ, Richards AE (1983) Experimental studies of the impact resistance of steel-faced concrete composites. 7th S.M.I.R.T. Conference, Paper J8/4
124. Kojima I, Kunita J, Tanaka N (1991) Experimental study of local behavior of reinforced concrete plates to missile impact. Nucl Eng Des 130(2):121–132. https://doi.org/10.1016/0029-5493(91)90121-W
125. Tsubota H, Kasai Y, Koshika N, Morikawa H, Uchida T, Ohno T (1993) Quantitative studies in impact resistance of reinforced concrete panels with steel liners under impact loading, part 1: scaled model impact tests. In: Kussmaul K, (Ed.), Proceedings of 12th International Conference on international association for structural mechanics in reactor technology (SMIRT). Stuttgart, Germany: Elsevier Science Publishers B.V.: 169–73
126. Hashimoto J, Takiguchi K, Nishimura K, Matsuzawa K, Tsutsui M, Ohashi Y (2005) Experimental study on behavior of RC panels covered with steel plates subjected to missile impact. In: Suyuan YU, (Ed.) Proceedings of 18th International Conference on international association for structural mechanics in reactor technology (SMIRT). Beijing, China
127. Dancygier AN, Katz A, Benamou D, Yankelevsky DZ (2014) Resistance of double-layered reinforced HPC barriers to projectile impact. Int J Impact Eng 67:39–51. https://doi.org/10.1016/j.ijimpeng.2014.01.001
128. Song D, Tan Q, Zhan H, Liu F, Jiang Z (2019) Experimental investigation on the cellular steel-tube-confined concrete targets against projectile impact. Int J Impact Eng 131:94–110. https://doi.org/10.1016/j.ijimpeng.2019.05.004

Publisher's Note Springer Nature remains neutral with regard to jurisdictional claims in published maps and institutional affiliations.